

Nitric oxide depresses connexin 43 after myocardial infarction in mice

P. E. M. Jackson,¹ Q. P. Feng^{1,2,3} and D. L. Jones^{1,2,3}

¹ Departments of Physiology & Pharmacology, University of Western Ontario, London, ON, Canada

² Department of Medicine, University of Western Ontario, London, ON, Canada

³ Lawson Health Research Institute, London, ON, Canada

Received 2 January 2008,
revision requested 24 January
2008,
revision received 10 March 2008,
accepted 27 March 2008
Correspondence: D. L. Jones,
Departments of Physiology &
Pharmacology, University of
Western Ontario, London, ON,
Canada N6A 5C1. E-mail:
dougjones@schulich.uwo.ca

Abstract

Aims: Heart failure (HF) is a major cause of death and morbidity. Connexin 43 (Cx43) content is reduced in the failing myocardium, but regulating factors have not been identified. In HF, inducible nitric oxide synthase (iNOS)-induced high levels of nitric oxide (NO) cause apoptosis and cardiac dysfunction. However, a direct iNOS–Cx43 link has not been demonstrated. We investigated this relationship in mice after myocardial infarction.

Methods: Effects of myocardial infarction were evaluated 2 weeks after coronary artery ligation in wild-type C57BL/6 (WT) and iNOS^{-/-} knockout mice. Myocardial Cx43 and Cx45 content were assessed by immunofluorescence confocal imaging and western blotting. Cardiac function was evaluated in anaesthetized mice using a micro pressure-tipped catheter inserted into the left ventricle.

Results: Despite similar infarct size, deficiency in iNOS resulted in significantly lower plasma nitrate/nitrite levels, better haemodynamic performance and lower mortality 2 weeks after coronary ligation. Myocardial Cx43, but not Cx45, content was lower in WT mice following ligation. The reduction in Cx43 was less in iNOS^{-/-} compared with WT mice. To assess the direct effect of NO on Cx43 expression, cultured neonatal mouse cardiomyocytes were employed. Incubation with the NO donor, *S*-nitroso-*N*-acetylpenicillamine, elicited a dose-dependent decrease in Cx43 content in cultured neonatal cardiomyocytes.

Conclusions: Increased NO production from iNOS depressed cardiac performance and contributed to the decreased myocardial Cx43 content 2 weeks after myocardial infarction.

Keywords connexins, gap junctions, heart failure, iNOS, nitric oxide.

In North America, approx. 1% of the population has heart failure (HF). This proportion is expected to increase as the population ages (Masoudi *et al.* 2003), and is predicted to be the leading cause of all disabilities (Murray & Freeman 1996, Pearson 1999). Mortality, with pump dysfunction and arrhythmia having approximately equally incidence, is unacceptably high (Kannel 1997). Cardiac remodelling and collagen build-up

isolate myocytes, and alter cardiac conduction (Weber *et al.* 1990), which is exacerbated by alterations in ventricular gap junction protein, connexin 43 (Cx43) content and distribution (Luque *et al.* 1994, De Mello 1999, Chen & Jones 2000, Brower & Janicki 2001, Dupont *et al.* 2001). Reduced gap junction plaque dimension and numbers have been correlated with increased arrhythmia in dogs and patients with HF

(Spach *et al.* 2000, Severs *et al.* 2004). However, mechanisms by which gap junction function is reduced in the failing myocardium remain poorly understood.

Nitric oxide (NO) is produced in the body catalysed by three nitric oxide synthase (NOS) enzymes. Endothelial NOS (eNOS, NOS3) and neuronal NOS (nNOS, NOS1) are calcium sensitive and constitutively active while inducible NOS (iNOS, NOS2) is calcium insensitive. Normal NO levels are regulated by the constitutive forms, eNOS and nNOS, which regulate blood pressure and cardiac function (Moncada *et al.* 1991, Kelly *et al.* 1996). Studies have shown that eNOS protects the heart from ischaemic injury (Sumeray *et al.* 2000). In contrast, high levels of NO resulting from the production by iNOS may harm healthy cells (Moncada *et al.* 1991, Lu *et al.* 2006). Cardiac myocytes have increased iNOS activity and protein in HF, which results in dramatically increased circulating NO levels (Haywood *et al.* 1996, Drexler *et al.* 1998, Vejlstrup *et al.* 1998, Feng *et al.* 1999, 2001, Heymes *et al.* 1999). This increased NO depresses contractility directly and/or through the formation of peroxynitrite-induced myocardial damage (Feng *et al.* 2001, Lancel *et al.* 2004), while blockade of iNOS activity reduced myocardial dysfunction and infarct size in the rat (Wang *et al.* 1999).

Heterozygous mice with deletion of the Cx43 gene have slowed conduction and enhanced ischaemia-induced arrhythmia, suggesting an important role of Cx43 in the regulation of cardiac rhythm (Lerner *et al.* 2000). In HF, Cx43 is reduced (Chen & Jones 2000, Kanno *et al.* 2003) and is redistributed within myocytes (Chen & Jones 2000), contributing to depressed pump function and arrhythmia. Also, Cx43 may be rendered non-functional through dephosphorylation (Beardslee *et al.* 2000). However, a direct relationship has not been shown between iNOS-produced NO and gap junction alterations. The present study tested the hypothesis that after myocardial infarction, depressed contractility and conduction are due, at least in part, to iNOS activation and NO-induced reduction in ventricular Cx43 content.

Methods

Animals and surgery

All experiments were approved by the University of Western Ontario Animal Care Committee and followed the Guidelines of the Canadian Council on Animal Care. Wild-type (WT) C57BL/6 and iNOS^{-/-} knockout mice (C57BL/6 background; Jackson Laboratories, Bar Harbor, ME, USA) of approx. 4 months of age were randomly assigned to one of three groups: (1) control, no surgery, (2) sham ligation surgery studied at 2 weeks, and (3) left main coronary artery ligation studied at 2 weeks (HF).

Induction of HF

Myocardial infarction was induced in mice as previously described (Feng *et al.* 2001). Briefly, the animal was anaesthetized with pentobarbital (35 mg kg⁻¹, Somnotol; MTC Pharmaceuticals, Cambridge, ON, Canada). A 23 ga endotracheal tube was inserted to assist respiration using a small animal respirator set at 90 beats min⁻¹. The chest was opened through a left lateral thoracotomy and an 8-0 silk suture was tied around the left main coronary artery. For sham operations, the suture was not placed. The chest was closed and respiration was maintained with 30 mm H₂O positive end expiratory pressure for 30 min until the mouse was breathing spontaneously. Buprenorphine analgesic was administered every 8 h during the first 2 days of recovery. Surgical loss was defined as death within 24 h of surgery. Ligation-induced deaths were recorded starting from 24 h after surgery until the study day. In surviving animals, blood samples were obtained and frozen at -80 °C for later analysis. The hearts were then removed, weighed and sectioned. The basal section, free of infarcted tissue, was weighed and frozen in liquid nitrogen and stored at -80 °C until used for western blotting. The apical portion containing the infarct was fixed in 4% paraformaldehyde for up to 1 month before immunostaining.

Haemodynamic measurements

To assess cardiac performance, mice from each group were anaesthetized with a mixture of ketamine (100 mg kg⁻¹) and xylazine (10 mg kg⁻¹). Through a cut down in the neck the jugular vein was cannulated with PE-10 tubing for drug administration and a 1.2 F microtip pressure sensor transducer catheter (Scisense, London, ON, Canada) was inserted through the left carotid artery into the left ventricle. The output from the pressure system was passed to a recording system mounted in a PC (EMKA Instruments, White Plains, VA, USA) with data analysed by the iOX software package (EMKA). After a 15-min stabilization period, haemodynamics were assessed with subsequent addition of dobutamine (0.03, 0.1 and 0.3 µg mL⁻¹) (Feng *et al.* 2001). At the end of the study, the hearts were removed and weighed; a section of viable ventricle was quickly frozen in liquid nitrogen, and then stored at -80 °C until being processed for Cx protein.

Plasma nitrate/nitrite

To determine NO production, the concentration of plasma nitrate/nitrite was determined using the Griess reaction (Grisham *et al.* 1996, Krieglstein *et al.* 2001). Nitrate is converted to nitrite using Aspergillus nitrate

reductase and then photometrically determined using the Sigma nitrate/nitrite kit (Sigma, St Louis, MO, USA) compared to a standard curve generated with serially diluted NaNO₃.

Immunostaining of Cx43

After routine paraffin imbedding of the heart tissue, and sectioning at 10 µm every 300 µm, sections were mounted on Superfrost Plus[®]-coated glass slides (Fisher Scientific, Nepean, ON, Canada). Slides were encircled with a grease pencil, deparaffinized and incubated with 0.1% trypsin to expose epitopes. Sections were blocked in a 3% bovine serum albumin (BSA)-buffered PBS solution for 45 min, then incubated with 80 µL of rabbit anti-Cx43 primary antibody (1 : 500 in PBS–BSA; Sigma). After washing in PBS, they were incubated in 40 µL of Texas Red[®]-conjugated goat anti-rabbit IgG (H&L; Cedarlane Lab, Hornby, ON, Canada, 1 : 30 in PBS–BSA). Sections were washed and mounted with Vectashield[®] (Vector Lab, Burlingame, CA, USA), and a cover slip was applied. Immunostained controls had sections incubated with the secondary antibody alone.

Confocal microscopy

Immunostained preparations were viewed on a laser scanning confocal microscope [Zeiss LSM 410 equipped with Kr/Ar and He/Ne lasers (Zeiss, Whiteplains, NY, USA)]. The Texas Red signal was excited with the Kr/Ar 568 nm line and viewed after passage through the LP 590 filter set using an oil immersion 63× objective lens. In addition to observing Cx43 distribution, an estimate of Cx43 content was obtained by assessing the number of pixels in each line of a line scan with intensities above baseline value set at 63 units, consistent with visualized Cx43, in 20 arbitrarily chosen fields from the non-infarcted zone of each of six preparations from each group (Darrow *et al.* 1996, Poelzing *et al.* 2004).

Infarct size determination

Slides adjacent to those used for confocal microscopy were stained with Mason's trichrome (Lee & Torack 1968, Lynch *et al.* 1976) for the assessment of infarct size as previously described (Feng *et al.* 2001). Stained slides were scanned on a Scanjet 7400c HP scanner (Hewlett-Packard, Mississauga, ON, Canada), and images transferred to PHOTOSHOP 7.0 (Adobe System, San Jose, CA, USA). A line was drawn on the endocardial surface of the infarct boarder using the 'Lasso' option. This line was transferred to a new image and formed into a circle and the software calculated the number of pixels inside the circle. This process was repeated for the non-infarcted zone. The sum of all the

zones was calculated as a stacked cone with the interzone distance corresponding to the intersection distance of 300 µm. The per cent of the infarcted zone in the apical part of the heart was calculated. The overall infarct size was then calculated based on the ratio of the weight of the ventricle and that of the apical portion.

Cell culture

To determine the direct effects of high levels of NO on Cx43 content, neonatal mouse cardiac myocyte cell cultures were incubated for 8 h with and without 10 and 100 µM of the NO donor, *S*-nitroso-*N*-acetylpenicillamine (SNAP; Sigma) (Song *et al.* 2000, Uchiyama *et al.* 2002). Briefly, hearts were removed from neonates within 24 h of birth, minced in nominally Ca²⁺- and Mg²⁺-free Hanks balanced solution (Sigma). Cardiomyocytes were dispersed by incubation with 0.625 mg mL⁻¹ collagenase (type II; Worthington Biochemicals, Freehold, NJ, USA), at 37 °C for 40 min. The suspension was centrifuged at 200 g for 5 min to obtain a cell pellet. Cells were then resuspended in M199 medium (Sigma), supplemented with 5% fetal calf serum (Sigma) and 5 mM D-glucose. Individual Petri dishes were pre-coated with 1% gelatine, autoclaved and left in an incubator [Model MCO-18AIC (UV); Sanyo Canada, Concord, ON, Canada] at 37 °C and 95% O₂ : 5% CO₂ for an hour before cells were plated. Cells were pre-plated for 2 h and washed to remove non-adhered myocytes and fibroblasts. Cardiac myocytes were then plated in 35 mm Petri dishes at a density of 2 × 10⁶ cells mL⁻¹ in M199, supplemented with 10% FCS and left for 48 h with the medium replaced with fresh medium at 24 h. The medium was then replaced with fresh medium for an 8-h incubation with or without SNAP. Cell viability was assessed at the end of the 8-h incubation by Trypan blue exclusion from triplicate samples from the control and 100 µM incubations.

Western blotting

Using routine procedures (Chen & Jones 2000), LV myocardium and cultured cardiomyocytes were homogenized. Protein concentrations were determined using the Lowry kit (Sigma). Twenty microgram protein per lane from LV myocardium or 30 µg from neonatal cell cultures were loaded and separated on 8% SDS-polyacrylamide gel, then electrophoretically transferred to nitrocellulose paper. After blocking in 5% Carnation[®] non-fat milk powder (Nestlé, Chesterille, ON, Canada) (overnight at 4 °C), membranes were incubated in rabbit anti-Cx43 primary antibody [1 : 14 000, 1 h at room temperature (RT); Sigma], then

incubation in horseradish peroxidase-conjugated goat anti-rabbit IgG (HRP-IgG, H&L; Cedarlane, 1 : 10 000, 1 h at RT). For Cx45, the primary antibody was rabbit anti-Cx45 (1 : 800; Chemicon International, Temecula, CA, USA), followed by HRP IgG (1 : 18 000). Anti-actin monoclonal antibody (1 : 5000; Chemicon), followed by goat anti-mouse HRP IgG (1 : 18 000; Bio-Rad), was used as loading control. For evaluation of phosphorylation, an additional set of blots were first probed for total Cx43 (as described above), then stripped and re-probed with the antibody specific for phosphorylation as the Ser368 site (1 : 1000; Chemicon) followed by redetection. Content was detected using enhanced chemiluminescence captured on Hyperfilm ECM (Amersham Life Sciences, London, ON, Canada) or determined by an optical reader (GelDoc; Bio-Rad). Data are expressed as a ratio of actin.

Statistical analysis

Data were analysed using one-way or two-way ANOVA (SPSS), followed by Bonferroni's *post-hoc* test and paired or unpaired Student's *t*-test (Sokal & Rohlf 1981), as appropriate. Kaplan–Meier analysis for mouse survival was performed using MedCalc (<http://www.medcalc.be>). A probability level of 5% was considered statistically significant.

Results

Infarction, survival and cardiac function

Infarct size produced by ligation of the left main coronary artery resulted in infarctions of approx. 35% of the anterior left ventricle with replacement of myocytes with scar and thinning of the ventricular wall evident at 2 weeks following ligation. Infarct size was similar between WT ($34 \pm 8\%$) and *iNOS*^{-/-} ($40 \pm 8\%$) in the surviving mice assessed at 2 weeks. Infarction induced significant mortality in both groups (Fig. 1); however, the *iNOS*^{-/-} mice had statistically lower mortality. Haemodynamics were depressed in WT mice with coronary artery ligation and their response to dobutamine was blunted compared with the sham-operated WT mice (Table 1, Fig. 2). This was most evident for the maximum developed pressure (Table 1) and the contractility (dP/dt_{\max} , Fig. 2). Indeed some of the WT HF mice did not tolerate the highest dose of dobutamine and did not survive this dose. The data from mice that did not survive the highest dose were not included in the data analysis. In the infarcted mice which did survive the highest dose, but of interest with lower pressure, contractility and relaxation changes, their mean heart rate decreased in the WT mice with infarction, while those of the sham-operated

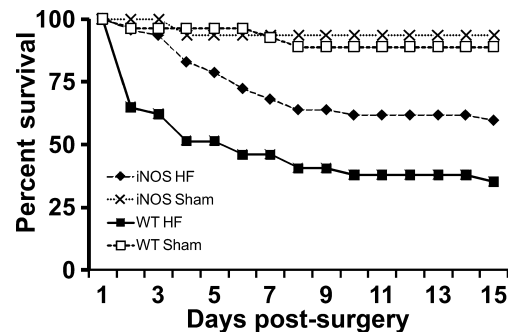


Figure 1 Kaplan–Meier analysis of post-ligation survival showing an overall significant mortality difference ($P > 0.0001$). The WT HF survival is also significantly less than that of the *iNOS*^{-/-}-HF group ($P = 0.006$). *iNOS*-HF ($n = 47$); *iNOS*-Sham ($n = 32$); WT HF ($n = 37$); WT Sham ($n = 27$). *iNOS*, *iNOS*^{-/-} knockout mice; WT, C57BL/6 wild-type mice; HF, mice which had coronary artery ligation-induced myocardial infarction and early sign of heart failure; Sham, sham-operated mice.

mice increased from the 1.0 to 3.0 $\mu\text{g mL}^{-1}$ dose (Table 1). On the other hand, *iNOS*^{-/-} mice did not have depressed performance and some of the *iNOS*^{-/-} mice had enhanced responses to the highest dose of dobutamine compared with the sham-operated control *iNOS*^{-/-} mice (Table 1, Fig. 2). Two-way ANOVA had statistically significant group \times drug interactions (Table 1). The lack of an increase in end diastolic pressure in the WT HF mice also indicates that there may not have been sufficient time for diastolic increases in these surviving animals.

Plasma nitrate/nitrite

Circulating NO levels assessed as nitrate/nitrite at the end of the study, averaged $52.3 \pm 2.6 \mu\text{M}$ in plasma from sham-operated WT mice, which was not different from the content in *iNOS*^{-/-} mice with ($55.0 \pm 2.6 \mu\text{M}$) or without ($45.9 \pm 2.9 \mu\text{M}$) myocardial infarction. In contrast, the nitrate/nitrite content in WT mice with infarct-induced HF was 50% higher, averaging $77.4 \pm 2.2 \mu\text{M}$ ($P < 0.01$). This suggested an activation of the *iNOS* system, which persisted at 2 weeks following coronary ligation in WT mice only.

Immunolocalization of Cx43 in ventricular myocytes

Cx43 immunostaining from WT mice was localized primarily in the intercalated disc region (Fig. 3a). Infarction resulted in a pronounced reduction in immunostaining, which was not restricted to the intercalated disc region (Fig. 3b). The *iNOS*^{-/-} sham-operated animals had similar immunostaining located primarily in the intercalated disc region, but the

Table 1 Haemodynamics in wild-type (WT) and inducible nitric oxide synthase (iNOS^{-/-}) mice with bolus injections of dobutamine

Experimental groups	Drug dose				Significance		
	Baseline	0.3 µg mL ⁻¹	1.0 µg mL ⁻¹	3.0 µg mL ⁻¹	Group	Drug	Interaction
WT							
<i>P</i> _{max}							
Sham	92 ± 3	93 ± 2	101 ± 4	134 ± 7	*	***	ns
HF	92 ± 2	91 ± 2	96 ± 3	119 ± 5			
DP							
Sham	102 ± 5	100 ± 3	108 ± 4	138 ± 8	*	***	ns
HF	98 ± 3	98 ± 3	103 ± 3	122 ± 10			
EDP							
Sham	6 ± 1	8 ± 1	8 ± 1	9 ± 1	ns	ns	ns
HF	5 ± 2	8 ± 2	8 ± 2	11 ± 1			
HR							
Sham	310 ± 21	349 ± 8	367 ± 13	423 ± 8	ns	*	ns
HF	336 ± 20	381 ± 20	399 ± 22	314 ± 10			
LV +dP/dt							
Sham	7419 ± 464	7553 ± 83	8659 ± 486	12747 ± 393	*	***	ns
HF	6905 ± 216	7201 ± 348	7768 ± 388	10318 ± 612			
LV -dP/dt							
Sham	6501 ± 379	6164 ± 307	6509 ± 455	8627 ± 1050	ns	ns	ns
HF	6025 ± 273	6173 ± 350	6394 ± 358	8012 ± 449			
iNOS ^{-/-}							
<i>P</i> _{max}							
Sham	94 ± 2	98 ± 3	101 ± 2	116 ± 2	*	***	ns
HF	97 ± 6	98 ± 7	108 ± 8	150 ± 10			
DP							
Sham	91 ± 3	95 ± 3	98 ± 2	113 ± 3	ns	***	ns
HF	93 ± 5	93 ± 7	103 ± 7	142 ± 10			
EDP							
Sham	17 ± 4	17 ± 2	18 ± 2	19 ± 3	ns	ns	ns
HF	17 ± 3	19 ± 3	18 ± 2	24 ± 4			
HR							
Sham	258 ± 20	306 ± 23	318 ± 25	357 ± 24	ns	***	ns
HF	288 ± 13	326 ± 10	325 ± 14	374 ± 23			
LV +dP/dt							
Sham	5850 ± 384	6134 ± 407	7025 ± 455	9213 ± 722	*	***	ns
HF	5668 ± 323	5749 ± 379	6514 ± 456	10457 ± 726			
LV -dP/dt							
Sham	5234 ± 381	5088 ± 319	5420 ± 321	7161 ± 333	ns	ns	ns
HF	4978 ± 321	4709 ± 294	5099 ± 270	7358 ± 238			

WT heart failure (HF) *n* = 12. WT Sham, *n* = 7. iNOS^{-/-}-HF, *n* = 11. iNOS^{-/-}-sham, *n* = 4. *P*_{max}, maximum developed pressure (mmHg); DP, developed pressure (mmHg); EDP, peak diastolic pressure (mmHg); HR, peak heart rate; LV +dP/dt, maximum rate of left ventricular contraction (mmHg s⁻¹); LV -dP/dt, maximum rate of left ventricular relaxation (mmHg s⁻¹); comparison of sham to heart failure groups analysed by two-way ANOVA.

P* < 0.05; **P* < 0.001; ns, nonsignificant.

intensity was lower than that seen in the WT sham-operated mice (Fig. 3c). Infarction in the iNOS^{-/-} mice did not appear to have as pronounced an effect on the content or distribution of Cx43 as it did in the WT mice (Fig. 3d). Assessment of the number of pixels containing immunofluorescent signal showed that Cx43 fluorescence intensity was significantly

lower in both groups with infarction compared with their corresponding sham groups (Table 2). However, the fluorescence intensity was significantly higher in the iNOS^{-/-} compared with the WT HF mice (*P* < 0.05). In order to quantify and confirm these findings, ventricular tissue from each group was subjected to western blots.

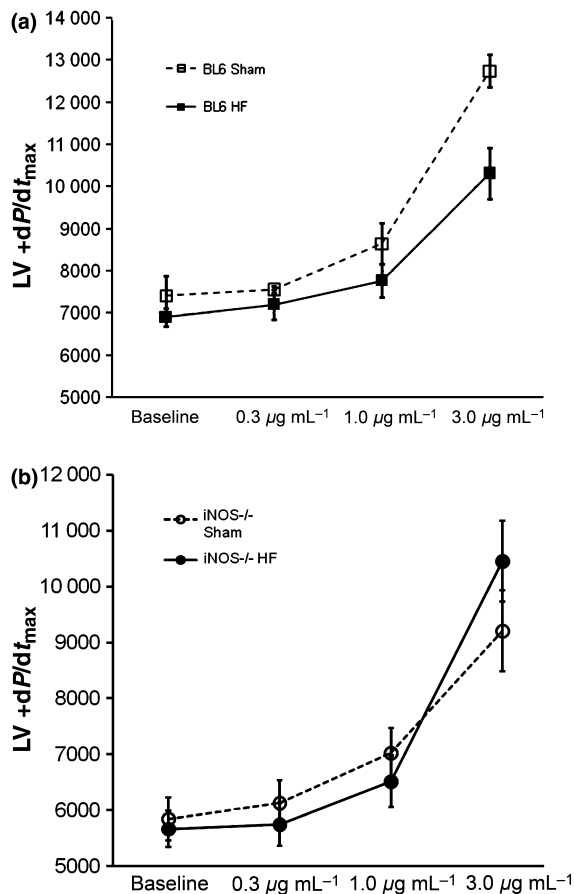


Figure 2 *In situ* determinations of contractility (LV dp/dt_{max}) rates in anaesthetized mice determined with injections of increasing doses of dobutamine. (a) Note the depressed dose-response in wild-type C57Bl/6 (BL6) mice with ligation-induced myocardial infarction (BL6 HF) compared with BL6 sham. (b) However, iNOS^{-/-} mice with similar coronary artery ligations (iNOS^{-/-} HF) did not have this depression.

The multiple Cx43 bands observed in western blots are reported as different phosphorylation states of Cx43, with the lowest band representing the non-phosphorylated protein (Beardslee *et al.* 2000, Ai & Pogwizd 2005). Therefore, the bands immunostained with the non-selective Cx43 antibody were reanalysed as an indirect index of phosphorylation (the top two bands) compared with the non-phosphorylated (lowest) band (Fig. 4a). There was a significant decrease in the phosphorylated Cx43 in WT HF compared with WT sham mice (Fig. 4c, $P < 0.05$), a decrease that was not present in the iNOS^{-/-} mice. Of note, there was a greater change in the ratio of phosphorylated to non-phosphorylated Cx43 in the WT HF mice (0.9) compared with the iNOS^{-/-} HF mice (1.4), suggestive of some protection from dephosphorylation in the iNOS^{-/-} mice. In addition, the ratio of phosphorylated to total Cx43 determined with the Ser 386 specific

antibody also revealed an approximately twofold higher ratio of phosphorylated to total Cx43 in the sham-operated (0.87 ± 0.2) vs. the WT HF mice (0.37 ± 0.1).

Heart failure-induced reductions in Cx43

Western blot analysis showed that there was an approx. 45% reduction in the amount of Cx43 in WT mice with infarction compared with the sham-operated WT mice (Fig. 4). However, there was a much smaller difference between sham and infarction in the iNOS^{-/-} mice, the decrease being approx. 22%. Also of note, the amount of Cx43 in the sham-operated iNOS^{-/-} mice was lower than that of the WT sham-operated animals. In separate samples with analysis of both Cx43 and Cx45, the Cx43 to actin ratio was also significantly lower (1.6 ± 0.25) in WT HF mice compared with sham-operated controls (4.4 ± 1.0 , $P < 0.05$). However, there was no significant difference in Cx45 content [1.0 ± 0.1 (HF) vs. 1.3 ± 0.2 (sham-operated)]. Similarly, Cx45 did not differ [1.3 ± 0.1 (HF) vs. 1.0 ± 0.1 (sham)] in iNOS^{-/-} mice.

Effects of SNAP on Cx43 protein in neonatal cardiomyocytes

To directly determine whether high levels of NO depress Cx43 protein content, cultured mouse neonatal cardiomyocytes were incubated for 8 h with 10 and 100 µM of the NO donor, SNAP. There was a highly significant, dose-related depression in Cx43 content with NO production (Fig. 5). The nitrate/nitrite levels were also measured in the culture medium and showed significant increases in NO_x levels from control (31.6 ± 3.1 µM) to 82.6 ± 4.6 µM with 100 µM SNAP, but of note, this was slightly higher than that found in plasma samples of mice with HF in this study (77.4 ± 2.2 µM). However, there were no differences in cell viability as assessed with Trypan blue exclusion (non-viable cells: $0.8 \pm 0.2\%$ in controls vs. $1.0 \pm 0.3\%$ in 100 µM SNAP treatment, $P = ns$).

Discussion

The main findings of this study were: (1) WT and iNOS^{-/-} knockout mice had decreased total content and altered distribution of Cx43 by 2 weeks after coronary artery ligation-induced infarction; (2) in contrast to iNOS^{-/-} knockout mice, WT mice had blunted haemodynamics despite similar infarct sizes; (3) Cx45 content was not altered following coronary artery ligation-induced infarction; (4) NO donor SNAP dose dependently decreased Cx43 content in neonatal mouse cardiac myocytes. These findings suggest that levels of

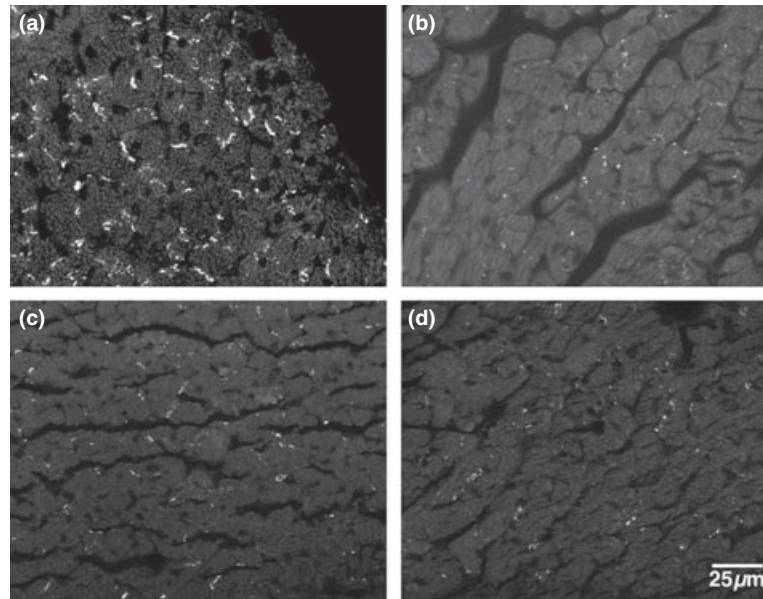


Figure 3 Confocal images of Cx43 in the ventricles of mice. (a) Section from C57BL/6 wild-type (WT) sham-operated mouse. Note the abundance of Cx43 immunostaining organized into plaques located in the intercalated disc regions. (b) WT with coronary artery-induced myocardial infarction. Note the reduction in immunostaining and the punctuate nature of the staining, which is distributed at sites throughout in the myocyte. (c) Immunostaining of iNOS^{-/-} sham mouse. Note the lower signal than the WT sham, but the connexins are organized into plaques. (d) The immunostaining from an iNOS^{-/-} mouse with infarct-induced myocardial infarction. Immunostaining is lower than that of the iNOS sham, but appears to be greater than that of the WT with coronary artery ligation-induced myocardial infarction.

Table 2 Fluorescence intensity peaks (arbitrary units) of Cx43 from immunofluorescence and confocal microscopy of paraffin-embedded mouse heart tissue of mice with sham or coronary artery ligation-induced myocardial infarction (heart failure, see Fig. 3) ($n = 6/\text{group}$)

Experimental group	Sham operated	HF
WT	91 ± 8	27 ± 3*
iNOS ^{-/-}	65 ± 6 [†]	40 ± 7 [†]

WT, wild-type; iNOS, inducible nitric oxide synthase.

* $P < 0.05$ compared with all other groups.

[†] $P < 0.05$ compared with the matched C57BL/6 (WT) group.

Two-way ANOVA had group, strain and interaction significance ($P < 0.05$).

NO produced by iNOS decrease the content and alter the distribution of the gap junction protein, Cx43, in the non-infarcted region of the left ventricle of mice by 2 weeks after coronary artery ligation. To the best of our knowledge, this is the first investigation to directly address a link between iNOS and Cx43 in the mouse model following coronary artery ligation.

The pronounced effects of myocardial infarction in the present study were confirmed by mortality and histology showing thinning of the ventricular wall with collagen deposition and chamber enlargement, consis-

tent with findings in patients and animals with HF and with our previous study with similar ligation-induced HF (Feng *et al.* 2001, Sam *et al.* 2001). The infarction sizes were similar among the groups, thus differences between groups are likely unrelated to infarct size. Plasma NO_x levels were higher in WT HF mice compared with sham-operated WT mice, but not in iNOS^{-/-} mice, despite similar sized infarcts.

There were differences in the baseline haemodynamic values between the iNOS^{-/-} and WT mice. The reason for these differences is not known. Because of these differences, it was important to determine effects within the strains separately. It was noteworthy that with the addition of dobutamine, the WT sham-operated mice achieved much higher values than those with coronary ligation. On the other hand, the iNOS^{-/-} mice with ligation did not fall below those of the shams. In addition, although there were pronounced depressions in contractility and relaxation in the surviving WT mice following coronary artery ligation-induced myocardial infarction, their end diastolic pressures were not different than those of the WT sham mice. This suggests that at 2 weeks the surviving mice were in the early stages of HF, exhibiting signs and symptoms of systolic but not diastolic HF, as observed by us using the same models, but allowed to survive for 4 weeks (Feng *et al.* 2001).

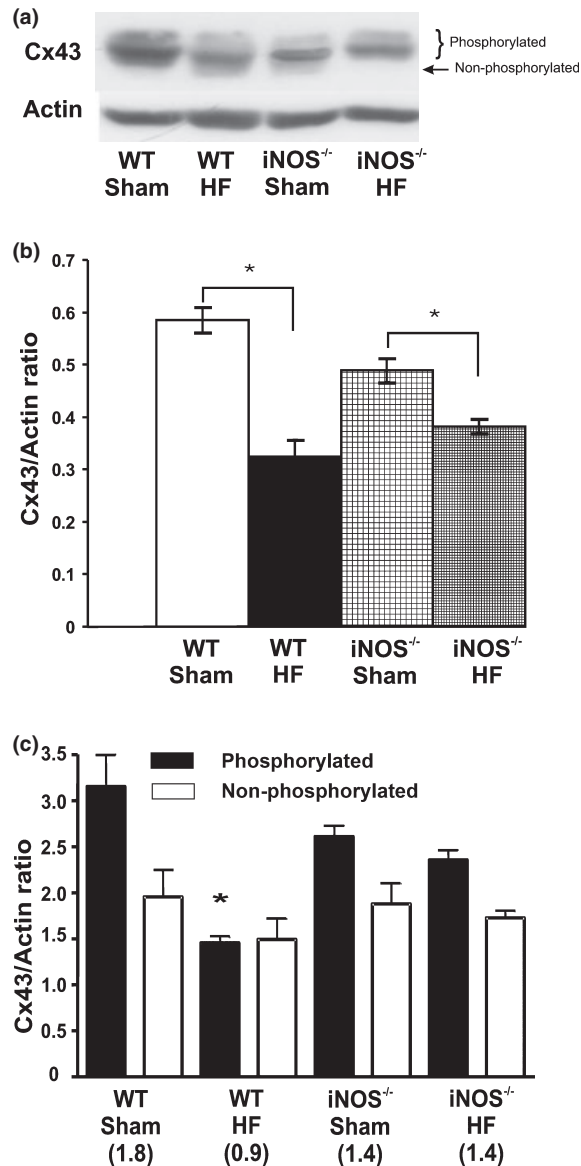


Figure 4 Total Cx43 content assessed from western blots (a), enlarged to show bands, expressed as ratio of Cx43 to actin from viable myocardium from wild-type (WT) and iNOS^{-/-} mice, with and without ligation-induced myocardial infarction 2 weeks after ligation or sham ligation (b). The ligation induced an approx. 50% decrease in Cx43 content in the WT mice, but only an approx. 20% decrease in the iNOS^{-/-} mice. ($n = 6$ per group, mean \pm SEM). In addition to the effects of ligation, there was a significant treatment and strain interaction ($*P < 0.05$, two-way ANOVA). (c) Bar graph of western blot analysis of phosphorylated and non-phosphorylated bands of Cx43 in WT and iNOS^{-/-} knockout mice, with sham operation or ligation-induced myocardial infarction (HF). Phosphorylated Cx43 was significantly lower in the WT HF mice than all other groups ($*P < 0.05$). Values in parentheses are the ratios of phosphorylated/non-phosphorylated within each group. WT, wild-type; iNOS^{-/-}, iNOS^{-/-} knockout mutants. HF, 2-week coronary artery ligation-induced myocardial infarction ($n = 6$ per group, mean \pm SEM).

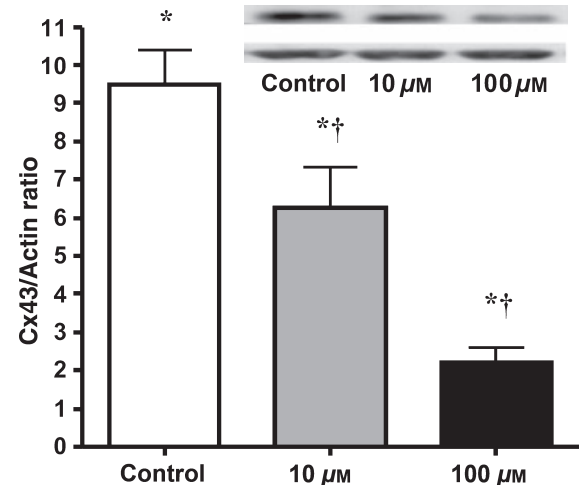


Figure 5 Bar graph of the effects of incubation of neonatal myocytes with S-nitroso-N-acetylpenicillamine (SNAP) for 8 h, which reduced Cx43 content in a dose-dependent manner. Cx43 is expressed as a ratio of Cx43 to actin in the sample, incubation in both 10 μ M (*, all groups were significantly different) and 100 μ M (†, 10 and 100 μ M groups were significantly different) SNAP significantly lowered Cx43 content in the myocytes. The inset shows a representative western blot for Cx43 (top) and actin (bottom) in each sample. ($n = 6$ per treatment, mean \pm SEM).

Gap junctions were confined mainly to the intercalated disc regions in the ventricles of sham-operated WT mice, consistent with that found in normal adult human left ventricular (LV) myocardium (Peters *et al.* 1993). With infarction, Cx43 signal was lower and scattered throughout the myocyte in the WT mice, similar to the change observed in the human LV myocardium following ischaemia or late-stage hypertrophy (Peters *et al.* 1993, Sepp *et al.* 1996, Kaprielian *et al.* 1998).

In the pacing-induced HF model in the canine (4–6 weeks), immunohistochemically identified Cx43 expression was strongly correlated with depressed conduction velocity assessed using high-resolution transmural optical mapping (Poelzing *et al.* 2004). Reduced Cx43 expression produced transmural uncoupling, slowed conduction and induced marked dispersion of repolarization, which was concluded to be arrhythmogenic (Poelzing *et al.* 2004). Ventricular arrhythmias have also been correlated with reduced Cx43 content in non-ischaemic dilated cardiomyopathic hearts from humans (Kitamura *et al.* 2002) and mice (Kanno *et al.* 2003).

Cx43 western blots had two to three obvious bands, which when identified by Cx-specific antibodies (Beardslee *et al.* 2000, Ai & Pogwizd 2005), differed in their phosphorylation: the upper and middle bands were phosphorylated, while the lower band was

non-phosphorylated (Beardslee *et al.* 2000, Ai & Pogwizd 2005). Although Cx43 phosphorylation has variable effects on intracellular communication (Darrow *et al.* 1996, Bowling *et al.* 2001), dephosphorylation has previously been shown to decrease gap junctional communication in neonatal rat ventricular cell pairs with activated endogenous phosphatases (Duthe *et al.* 2001) or in perfused whole rat hearts during acute ischaemia (Beardslee *et al.* 2000). In the present study, the content of the upper bands (presumed to be phosphorylated) and the ratio of the Ser368 phospho-specific to total Cx43 were significantly lower in WT HF mice compared with sham-operated WT mice. These findings are consistent with the decrease in both Cx43 expression and the proportion of phosphorylated Cx43 in rabbits and humans with non-ischaemic HF (Ai & Pogwizd 2005). In contrast, in the present study, there was no change in the phosphorylation ratio in the iNOS^{-/-} mice with coronary artery ligation-induced myocardial infarction, suggesting some degree of protection was afforded with the lack of iNOS.

To directly evaluate whether high levels of NO alter Cx43 content, cultured neonatal mouse cardiac myocytes were treated with the NO donor, SNAP, which produced a dose-dependent reduction in Cx43 protein content. In the present study, SNAP treatment for 8 h did not induce cell death as Trypan blue exclusion showed no difference in cell viability between control and incubation in the 100 μ M of SNAP. Also, NO_x levels in the culture medium from the neonatal mouse cardiomyocytes incubated in the highest levels of SNAP were only slightly above the range found in the plasma samples of mice with HF. Thus, these data show directly that high levels of NO, similar to those observed in HF, cause a reduction in Cx43 protein content.

A partial compensation for decreased Cx43 by slightly increased Cx45 content was found in patients with end-stage HF (Yamada *et al.* 2003). Interestingly, there were no changes in Cx45 mRNA, leading the authors to suggest that these changes were caused by reduced Cx45 degradation rather than altered transcription. In the present study, there was no change in Cx45 content. This may reflect species differences or the short time of the mouse model in this study and/or data only from surviving mice at 2 weeks compared with the findings from Yamada *et al.* (2003) in patients with end-stage HF. Whether longer duration would also have increased compensatory Cx45 content (Yamada *et al.* 2003) is unknown.

The reason for the slightly lower Cx43 immunostaining signal in sham-operated iNOS^{-/-} mice than WT mice is not apparent. The distribution of Cx43 was similar in both groups: located primarily along the intercalated discs. iNOS^{-/-} mice have decreased NF- κ B, JNK and AP-1 activity, which may have contributed to lower

Cx43 transcription (Mizukami *et al.* 1997). However, there was less of a drop in Cx43 protein content and the ratio of the phosphorylated to non-phosphorylated Cx43 was lower in WT than in iNOS^{-/-} mice with infarction. Overall, the effect of coronary artery ligation was considerably blunted in the iNOS^{-/-} knockout mice. Further, these findings support a link between iNOS-derived NO and Cx43 downregulation in HF.

The mechanisms responsible for these reductions in Cx43 are unknown, but may include: decreased transcription; increased internalization; failure to incorporate Cx43 into the cell membrane, and/or increased removal of gap junctions from the cell membrane (Laird & Revel 1990, Gros & Jongsma 1996). Modifying iNOS activity using selective iNOS blockers may reveal more information on the role of iNOS in Cx43 expression and may be a therapeutic option for patients with HF.

Limitations

No animal model mimics all the features of the patient with HF and direct extrapolation from these findings is not possible. However, animal models are essential to study progression of the disease process, which is virtually impossible to do in detail in patients such as those with HF in which the early stages are often unrecognized, and during the later stages there is an ethical requirement for treatment. The mouse has become the animal of choice because of its applicability for experiments requiring gene targeting. Caution is also warranted as results were obtained only from mice surviving to 2 weeks, and there may have been more pronounced or different responses in moribund animals or those surviving for longer periods of time, for example the lack of an increase in diastolic pressure in WT mice following coronary artery ligation-induced myocardial infarction. Finally, adult mouse cardiomyocytes are difficult to culture. Thus, neonatal myocyte cultures have become the standard for assessing factors responsible for protein expression as well as cellular biochemistry, but the neonatal cardiac myocyte is in a developmental and hypertrophic state, which is not identical to that of adult cardiomyocytes.

Conflict of interest

None of the authors have any conflicts of interest with regard to this paper.

This study was supported by the Canadian Institutes for Health Research (DLJ). P.E.M.J. was supported by a traineeship from the Heart and Stroke Foundation of Ontario Group Grant in Heart Failure. Special thanks are extended to Hongmei Zhao, Yahong Li, Waseem Iqbal and Xiangru Lu for excellent technical assistance.

References

- Ai, X. & Pogwizd, S.M. 2005. Connexin 43 downregulation and dephosphorylation in nonischemic heart failure is associated with enhanced colocalized protein phosphatase type 2A. *Circ Res* 96, 54–63.
- Beardslee, M.A., Lerner, D.L., Tadros, P.N., Laing, J.G., Beyer, E.C., Yamada, K.A., Kleber, A.G., Schuessler, R.B. & Saffitz, J.E. 2000. Dephosphorylation and intracellular redistribution of ventricular connexin43 during electrical uncoupling induced by ischemia. *Circ Res* 87, 656–662.
- Bowling, N., Huang, X., Sandusky, G.E., Fouts, R.L., Mintze, K., Esterman, M., Allen, P.D., Maddi, R., McCall, E. & Vlahos, C.J. 2001. Protein kinase C- α and - ϵ modulate connexin-43 phosphorylation in human heart. *J Mol Cell Cardiol* 33, 789–798.
- Brower, G.L. & Janicki, J.S. 2001. Contribution of ventricular remodeling to pathogenesis of heart failure in rats. *Am J Physiol Heart Circ Physiol* 280, H674–H683.
- Chen, M. & Jones, D.L. 2000. Age- and myopathy-dependent changes in connexins of normal and cardiomyopathic Syrian hamster ventricular myocardium. *Can J Physiol Pharmacol* 78, 669–678.
- Darrow, B.J., Fast, V.G., Kleber, A.G., Beyer, E.C. & Saffitz, J.E. 1996. Functional and structural assessment of intercellular communication. Increased conduction velocity and enhanced connexin expression in dibutyl cAMP-treated cultured cardiac myocytes. *Circ Res* 79, 174–183.
- De Mello, W.C. 1999. Cell coupling and impulse propagation in the failing heart. *J Cardiovasc Electrophysiol* 10, 1409–1420.
- Drexler, H., Kasmer, S., Strobel, A., Studer, R., Brodde, O.E. & Hasenfuss, G. 1998. Expression, activity and functional significance of inducible nitric oxide synthase in the failing human heart. *J Am Coll Cardiol* 32, 955–963.
- Dupont, E., Matsushita, T., Kaba, R.A., Vozzi, C., Coppen, S.R., Khan, N., Kaprielian, R., Yacoub, M.H. & Severs, N.J. 2001. Altered connexin expression in human congestive heart failure. *J Mol Cell Cardiol* 33, 359–371.
- Duthe, F., Plaisance, I., Sarrouilhe, D. & Herve, J.C. 2001. Endogenous protein phosphatase 1 runs down gap junctional communication of rat ventricular myocytes. *Am J Physiol Cell Physiol* 281, C1648–C1656.
- Feng, Q., Fortin, A.J., Lu, X., Malcolm, J. & Arnold, O. 1999. Effects of L-arginine on endothelial and cardiac function in rats with heart failure. *Eur J Pharmacol* 376, 37–44.
- Feng, Q., Lu, X., Jones, D.L., Shen, J. & Arnold, J.M. 2001. Increased inducible nitric oxide synthase expression contributes to myocardial dysfunction and higher mortality after myocardial infarction in mice. *Circulation* 104, 700–704.
- Grisham, M.B., Johnson, G.G. & Lancaster, J.R., Jr. 1996. Quantitation of nitrate and nitrite in extracellular fluids. *Methods Enzymol* 268, 237–246.
- Gros, D.B. & Jongsma, H.J. 1996. Connexins in mammalian heart function. *Bioessays* 18, 719–730.
- Haywood, G.A., Tsao, P.S., der Leyen, H.E., Mann, M.J., Keeling, P.J., Trindade, P.T., Lewis, N.P., Byrne, C.D., Rickenbacher, P.R., Bishopric, N.H., Cooke, J.P., McKenna, W.J. & Fowler, M.B. 1996. Expression of inducible nitric oxide synthase in human heart failure. *Circulation* 93, 1087–1094.
- Heymes, C., Vanderheyden, M., Bronzwaer, J.G., Shaw, A.M. & Paulus, W.J. 1999. Endomyocardial nitric oxide synthase and left ventricular preload reserve in dilated cardiomyopathy. *Circulation* 99, 3009–3016.
- Kannel, W.B. 1997. Epidemiology of heart failure in the United States. In: P.A. Poole-Wilson, W.S. Colucci, B.M. Massie, K. Chatterjee & A.J.S. Coates. (eds) *Heart Failure: Scientific Principles and Clinical Practice*, 1st edn, pp. 279–298. Churchill Livingstone Inc., New York.
- Kanno, S., Kovacs, A., Yamada, K.A. & Saffitz, J.E. 2003. Connexin43 as a determinant of myocardial infarct size following coronary occlusion in mice. *J Am Coll Cardiol* 41, 681–686.
- Kaprielian, R.R., Gunning, M., Dupont, E., Sheppard, M.N., Rothery, S.M., Underwood, R., Pennell, D.J., Fox, K., Pepper, J., Poole-Wilson, P.A. & Severs, N.J. 1998. Downregulation of immunodetectable connexin43 and decreased gap junction size in the pathogenesis of chronic hibernation in the human left ventricle. *Circulation* 97, 651–660.
- Kelly, R.A., Balligand, J.L. & Smith, T.W. 1996. Nitric oxide and cardiac function. *Circ Res* 79, 363–380.
- Kitamura, H., Ohnishi, Y., Yoshida, A., Okajima, K., Azumi, H., Ishida, A., Galeano, E.J., Kubo, S., Hayashi, Y., Itoh, H. & Yokoyama, M. 2002. Heterogeneous loss of connexin43 protein in nonischemic dilated cardiomyopathy with ventricular tachycardia. *J Cardiovasc Electrophysiol* 13, 865–870.
- Kriegelstein, C.F., Cerwinka, W.H., Laroux, F.S., Salter, J.W., Russell, J.M., Schuermann, G., Grisham, M.B., Ross, C.R. & Granger, D.N. 2001. Regulation of murine intestinal inflammation by reactive metabolites of oxygen and nitrogen: divergent roles of superoxide and nitric oxide. *J Exp Med* 194, 1207–1218.
- Laird, D.W. & Revel, J.-P. 1990. Biochemical and immunological analysis of the arrangement of connexin 43 in rat heart gap junction membranes. *J Cell Sci* 97, 109–117.
- Lancel, S., Tissier, S., Mordon, S., Marechal, X., Depontieu, F., Scherpereel, A., Chopin, C. & Neviere, R. 2004. Peroxynitrite decomposition catalysts prevent myocardial dysfunction and inflammation in endotoxemic rats. *J Am Coll Cardiol* 43, 2348–2358.
- Lee, S.H. & Torack, R.M. 1968. Aldehyde as fixative for histochemical study of glutamic oxaloacetic transaminase. *Histochemie* 12, 341–344.
- Lerner, D.L., Yamada, K.A., Schuessler, R.B. & Saffitz, J.E. 2000. Accelerated onset and increased incidence of ventricular arrhythmias induced by ischemia in Cx43-deficient mice. *Circulation* 101, 547–552.
- Lu, X., Hamilton, J.A., Shen, J., Pang, T., Jones, D.L., Potter, R.F., Arnold, J.M. & Feng, Q. 2006. Role of tumor necrosis factor- α in myocardial dysfunction and apoptosis during hindlimb ischemia and reperfusion. *Crit Care Med* 34, 484–491.
- Luque, E.A., Veenstra, R.D., Beyer, E.C. & Lemanski, L.F. 1994. Localization and distribution of gap junctions in normal and cardiomyopathic hamster heart. *J Morphol* 222, 203–213.

- Lynch, H.T., Saldivar, V.A., Guirgis, H.A., Terasaki, P.I., Bardawil, W.A., Harris, R.E., Lynch, J.F. & Thomas, R. 1976. Familial Hodgkin's disease and associated cancer. A clinical-pathologic study. *Cancer* **38**, 2033–2041.
- Masoudi, F.A., Havranek, E.P., Smith, G., Fish, R.H., Steiner, J.F., Ordin, D.L. & Krumholz, H.M. 2003. Gender, age, and heart failure with preserved left ventricular systolic function. *J Am Coll Cardiol* **41**, 217–223.
- Mizukami, Y., Yoshioka, K., Morimoto, S. & Yoshida, K. 1997. A novel mechanism of JNK1 activation. Nuclear translocation and activation of JNK1 during ischemia and reperfusion. *J Biol Chem* **272**, 16657–16662.
- Moncada, S., Palmer, R.M. & Higgs, E.A. 1991. Nitric oxide: physiology, pathophysiology and pharmacology. *Pharmacol Rev* **43**, 109–142.
- Murray, D.R. & Freeman, G.L. 1996. Tumor necrosis factor-alpha induces a biphasic effect on myocardial contractility in conscious dogs. *Circ Res* **78**, 154–160.
- Pearson, T.A. 1999. Cardiovascular disease in developing countries: myths, realities, and opportunities. *Cardiovasc Drugs Ther* **13**, 95–104.
- Peters, N.S., Green, C.R., Poole-Wilson, P.A. & Severs, N.J. 1993. Reduced content of connexin43 gap junctions in ventricular myocardium from hypertrophied and ischemic human hearts. *Circulation* **88**, 864–875.
- Poelzing, S., Akar, F.G., Baron, E. & Rosenbaum, D.S. 2004. Heterogeneous connexin43 expression produces electrophysiological heterogeneities across ventricular wall. *Am J Physiol Heart Circ Physiol* **286**, H2001–H2009.
- Sam, F., Sawyer, D.B., Xie, Z., Chang, D.L., Ngoy, S., Brenner, D.A., Siwik, D.A., Singh, K., Apstein, C.S. & Colucci, W.S. 2001. Mice lacking inducible nitric oxide synthase have improved left ventricular contractile function and reduced apoptotic cell death late after myocardial infarction. *Circ Res* **89**, 351–356.
- Sepp, R., Severs, N.J. & Gourdie, R.G. 1996. Altered patterns of cardiac intercellular junction distribution in hypertrophic cardiomyopathy. *Heart* **76**, 412–417.
- Severs, N.J., Dupont, E., Coppen, S.R., Halliday, D., Inett, E., Baylis, D. & Rothery, S. 2004. Remodelling of gap junctions and connexin expression in heart disease. *Biochim Biophys Acta* **1662**, 138–148.
- Sokal, R.R. & Rohlf, F.J. 1981. *Biometry: The Principles and Practice of Statistics in Biological Research*, 2nd edn. W. H. Freeman and Company, San Francisco, CA.
- Song, W., Lu, X. & Feng, Q. 2000. Tumor necrosis factor-alpha induces apoptosis via inducible nitric oxide synthase in neonatal mouse cardiomyocytes. *Cardiovasc Res* **45**, 595–602.
- Spach, M.S., Heidlage, J.F., Dolber, P.C. & Barr, R.C. 2000. Electrophysiological effects of remodeling cardiac gap junctions and cell size: experimental and model studies of normal cardiac growth. *Circ Res* **86**, 302–311.
- Sumeray, M.S., Rees, D.D. & Yellon, D.M. 2000. Infarct size and nitric oxide synthase in murine myocardium. *J Mol Cell Cardiol* **32**, 35–42.
- Uchiyama, T., Otani, H., Okada, T., Ninomiya, H., Kido, M., Imamura, H., Nogi, S. & Kobayashi, Y. 2002. Nitric oxide induces caspase-dependent apoptosis and necrosis in neonatal rat cardiomyocytes. *J Mol Cell Cardiol* **34**, 1049–1061.
- Vejlstrup, N.G., Bouloumie, A., Boesgaard, S., Andersen, C.B., Nielsen-Kudsk, J.E., Mortensen, S.A., Kent, J.D., Harrison, D.G., Busse, R. & Aldershvile, J. 1998. Inducible nitric oxide synthase (iNOS) in the human heart: expression and localization in congestive heart failure. *J Mol Cell Cardiol* **30**, 1215–1223.
- Wang, D., Yang, X.P., Liu, Y.H., Carretero, O.A. & Lapointe, M.C. 1999. Reduction of myocardial infarct size by inhibition of inducible nitric oxide synthase. *Am J Hypertens* **12**, 174–182.
- Weber, K.T., Pick, R., Silver, M.A., Moe, G.W., Janicki, J.S., Zucker, I.H. & Armstrong, P.W. 1990. Fibrillar collagen and remodeling of dilated canine left ventricle. *Circulation* **82**, 1387–1401.
- Yamada, K.A., Rogers, J.G., Sundset, R., Steinberg, T.H. & Saffitz, J.E. 2003. Up-regulation of connexin45 in heart failure. *J Cardiovasc Electrophysiol* **14**, 1205–1212.